ADVANCING EARTH AND SPACE SCIENCES

Geophysical Research Letters

RESEARCH LETTER

10.1029/2024GL114472

Optimized J2 Recovery for Multi-Decadal Geophysical Studies

B. D. Loomis[1], T. J. Sabaka[1], K. E. Rachlin[2], M. J. Croteau[1], F. G. Lemoine[1], R. S. Nerem[3], and A. Bellas-Manley[3]

[1]Geodesy and Geophysics Laboratory, NASA Goddard Space Flight Center, Greenbelt, MD, USA, [2]KBRwyle, Greenbelt, MD, USA, [3]University of Colorado, Boulder, CO, USA

Key Points:

- The long-term J_2 time series is a unique climate data record that informs glacial isostatic adjustment models, length of day changes, and ice and ocean mass change
- Previous studies have shown the sensitivity of J_2 estimates to the modeled time variable gravity (TVG), only available with GRACE and GRACE-FO
- J_2 is recovered without TVG models using truncated singular value decomposition and only higher altitude satellite laser ranging satellites

Supporting Information:

Supporting Information may be found in the online version of this article.

Correspondence to:

B. D. Loomis,
bryant.d.loomis@nasa.gov

Citation:

Loomis, B. D., Sabaka, T. J., Rachlin, K. E., Croteau, M. J., Lemoine, F. G., Nerem, R. S., & Bellas-Manley, A. (2025). Optimized J2 recovery for multi-decadal geophysical studies. *Geophysical Research Letters*, *52*, e2024GL114472. https://doi.org/10.1029/2024GL114472

Received 24 DEC 2024
Accepted 8 MAR 2025

Abstract The time history of the Earth's dynamic oblateness, or J_2, is a unique climate data record, with its estimation from satellite laser ranging (SLR) tracking data beginning in 1976. Due to its impact on variations in length of day (LOD), the long-term J_2 time series is frequently applied to LOD studies and their contributions, which include tidal friction, glacial isostatic adjustment, ice melt, sea level change, and the angular momentum exchange between the fluid outer core and the mantle. Previous studies demonstrated that the accurate recovery of J_2 requires the use of time variable gravity models from GRACE when processing the SLR tracking data. However, no reliable models exist prior to GRACE's 2002 launch, calling into to question the accuracy and utility of the pre-GRACE estimates. Here we present a new approach to accurately recover J_2 without gravity modeling, resulting in the first fully consistent long-term solution for climate studies.

Plain Language Summary The Earth's dynamic oblateness, known as J_2, is a measure that reflects changes in the Earth's shape and affects how the length of a day changes. This measurement has been tracked using satellite data since 1976. Scientists use J_2 data to study various factors like tidal friction, changes in the Earth's crust, ice melt, sea level changes, and the interaction between the Earth's outer core and mantle. Recent work has shown that J_2 estimates before the GRACE satellite mission started in 2002 are not reliable because accurate gravity models are not available. This study introduces a new method for measuring J_2 without relying on these gravity models, providing a more consistent long-term data set for climate research and analysis.

1. Introduction

Temporal variability in the Earth's gravity field as observed by the Gravity Recovery and Climate Experiment (GRACE, 2002–2017) and GRACE Follow-On (GRACE-FO, 2018-Present) missions is caused by a variety of geophysical processes involving the movement of mass in the hydrosphere, cryosphere, ocean, atmosphere, and solid Earth. The largest and longest observed component of the time variable gravity (TVG) field is the dynamic oblateness, described by the spherical harmonic coefficient C_{20}, or its unnormalized form, J_2, which is equal to $-C_{20}\sqrt{5}$. The most accurate estimates are determined with satellite laser ranging (SLR) tracking data, which has been employed for the determination of C_{20} as far back as 1976 (Cheng et al., 2013). SLR gravity estimation commonly utilizes tracking data to a set of spherical satellites equipped with laser retro-reflectors, where their orbital configurations and material properties lead to differing contributions to the estimated spherical harmonic coefficients (Cheng & Ries, 2017; Sośnica et al., 2015; Tucker et al., 2022). GRACE-FO Technical Note 14 (TN-14) (Loomis et al., 2020), which contains SLR-derived estimates of C_{20} and C_{30} over the GRACE era, currently utilizes tracking data to the three Medium Earth Orbit (MEO) satellites LAGEOS-1 (1976 Launch), LAGEOS-2 (1992), LARES-2 (2022), and the five Low Earth Orbit (LEO) satellites Starlette (1975), AJISAI (1986), Stella (1993), Larets (2003), and LARES (2012) (See Table S1 in Supporting Information S1 for SLR satellite information). It is generally recommended that the SLR-derived values replace the GRACE and GRACE-FO estimates of C_{20} for the full data record and C_{30} for months where only one accelerometer is available (Loomis et al., 2020).

The release of TN-14 followed the analysis of Loomis et al. (2019), which demonstrated that C_{20} estimates are highly dependent on the choice of background gravity model used when processing the SLR tracking data, and that improved accuracy is achieved by using GRACE TVG information (other than C_{20}) to mitigate the negative impacts of correlations between the adjusted gravity coefficients. Consequently, the operational TN-14 processing utilizes the most recent Level 2 GRACE-FO solution to update the TVG model each month. While this approach is highly successful for the accurate recovery of C_{20} during the GRACE/-FO record, it highlights the

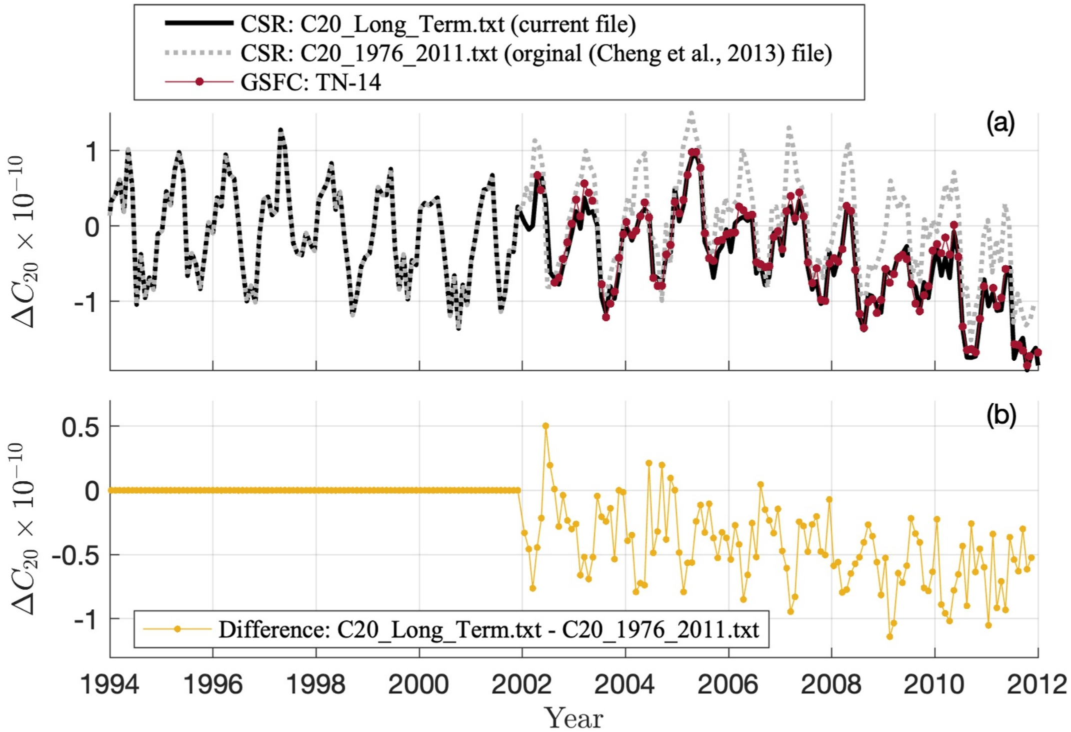

Figure 1. (a) Comparison of long-term ΔC_{20} solutions produced by Center for Space Research (CSR) and Goddard Space Flight Center (GSFC) Technical Note 14 (TN-14). Note that the AOD1B RL06 product (Flechtner, 2007) used in the GSFC processing has been removed from the two CSR solutions. (b) The discrepancy between the current and original CSR files is due to a change in time variable gravity modeling introduced in 2002. The relative bias offset for TN-14 is selected to provide the best agreement to C20_Long_Term.txt.

critical importance of developing an approach to estimate C_{20} without TVG, in order to produce reliable estimates from 1976 to the launch of GRACE in April 2002, and during gaps in the GRACE/-FO data record. Note that we are not concerned with C_{30} in this study, as it is not well-recovered by SLR until the launch of LARES in 2012 (Loomis et al., 2020). The effect of TVG modeling on SLR-derived C_{20} estimates can be quite large, as demonstrated by Loomis et al. (2019), who report a 38% change in C_{20} trend for 2005–2015 when comparing TN-11 (the standard at the time that did not include TVG) to our recommended solution that includes TVG. This level of trend error is an order of magnitude larger than the ~3% uncertainty (1-σ) reported by Cheng et al. (2013), for 1976–1992 ($\dot{J}_2 = -3.7 \pm 0.1 \times 10^{-11}$/yr), the portion of the record with the least and lowest quality of data.

The large impact of TVG and the importance of consistent modeling on estimates of C_{20} is further illustrated in Figure 1, which presents the TN-14 solution produced by the NASA Goddard Space Flight Center (GSFC), along with two different long-term C_{20} solutions produced by the University of Texas Center for Space Research (CSR). The original file distributed with (Cheng et al., 2013) did not include any TVG information, while the file currently being distributed matches the original C_{20} solution until 2002, at which point GRACE-derived TVG is introduced into the background model (Ries, 2024). While the inclusion of TVG during the GRACE/-FO record leads to very good agreement with TN-14, it creates a significant inconsistency in the solution, as illustrated in the bottom panel of Figure 1, which shows the differences between the current and original long-term CSR C_{20} products. This leads to the obvious question that arises when examining Figure 1 and the conclusions of Loomis et al. (2019): If we must use TVG modeling to properly recover C_{20} during the GRACE era, how can we trust the C_{20} estimates during the pre-GRACE era when no such TVG information is available? The C_{20} time history of (Cheng et al., 2013) is highly cited and has been applied to a wide range of geophysical studies, including the examination and quantification of length-of-day (LOD) variations, glacial isostatic adjustment (GIA), and long-term changes in ice and ocean mass (e.g., Agnew, 2024; Mitrovica et al., 2015; Nerem & Wahr, 2011; Shahvandi et al., 2024), but the validity of those studies and their conclusions hinge on the reliability of the long-term C_{20}

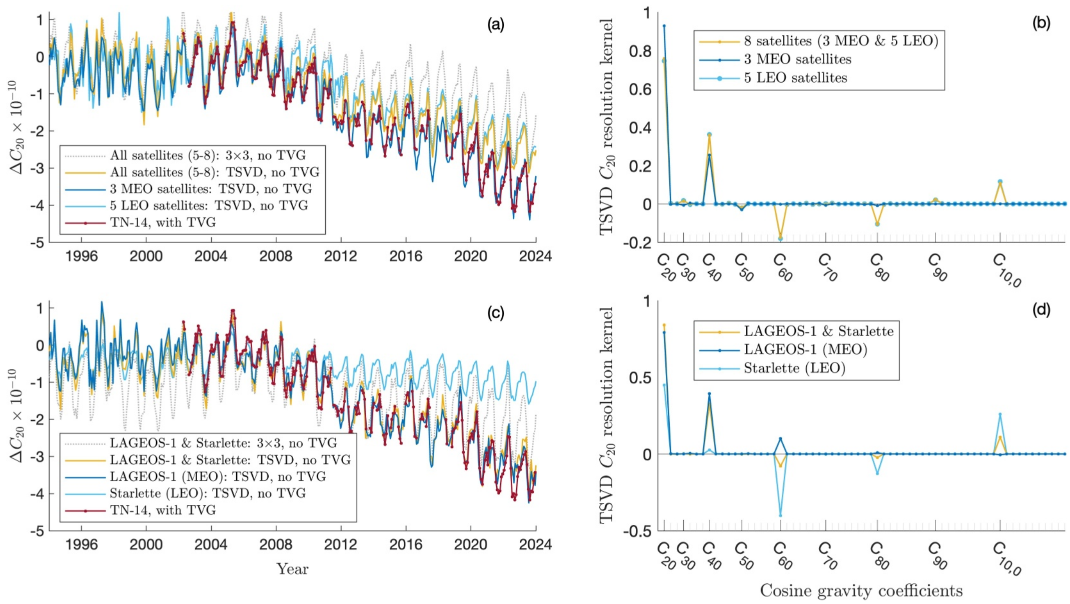

Figure 2. (a), (c) ΔC_{20} time series for various solutions. (b), (d) C_{20} resolution kernels for the Truncated Singular-Value Decomposition (TSVD) solutions, where the cosine coefficients, C_{nm}, on the x-axis are arranged by degree, n, and order, m. The C_{20} leakage into all sine coefficients, S_{nm}, is negligible and so is not shown. (a)–(b) Results for all 5–8 satellites available 1993–Present. (c)–(d) Results for only the two satellites available in 1976. (b) Resolution kernels are shown for January 2024, when all 8 satellites are available. (d) The mean averaging kernel for the full time span is shown. This analysis (a)–(d) demonstrates the superior performance of the TSVD applied to the Medium Earth Orbit satellites only.

solution. The average rate of change for the earliest years (e.g., 1976–1991) has been of particular interest for constraining and validating the lower mantle viscosity (Argus et al., 2021; Mitrovica et al., 2015).

The primary goal of this study is to develop a methodology that is able to recover C_{20} without TVG modeling, in order to provide a consistent and accurate solution from 1976–Present that is suitable for multi-decadal climate studies and constraining GIA models. Following the convention in recent publications, we will present time series of C_{20}, but report regression fit parameters (e.g., trends) in terms of J_2.

2. Data and Methods

2.1. SLR Data Processing

SLR data processing and orbit determination procedures are adopted from prior work described in (F. G. Lemoine et al., 2006; Zelensky et al., 2014; Loomis et al., 2019). For 1993–2024, we utilize the normal point tracking data for the 5–8 SLR satellites listed in the Introduction and Table S1 in Supporting Information S1 to generate normal equations for a 10×10 gravity expansion in 7-day increments (i.e., arcs). Note that for TN-14, which is available 2002–2024, we limit the adjusted gravity parameters to $5 \times 5 + C_{61}/S_{61}$ (Cheng & Ries, 2017), apply TVG modeling (Loomis et al., 2019), and then combine four 7-day arcs to produce gravity estimates from 28 days of data. For the span 1993–2024, we apply processing and estimation strategies that have been refined by our group over many years to produce optimal orbits. This includes dynamic data editing and station measurement bias estimation, where the a priori biases follow the recommendations of the International Laser Ranging Service (ILRS). However, these well-established procedures do not perform as well for the earliest SLR data due to a variety of reasons, including a sparse station network, fewer satellites, and early generation station hardware with reduced accuracy. We have identified three data processing strategies that successfully mitigate the noise in our C_{20} estimates for the pre-1993 data: (a) we extend the arc length to 56 days, (b) we estimate simple measurement biases per station per arc, and (c) we are less aggressive with our data editing to retain enough tracking data. Regarding the first strategy, we note that we apply 56-day arcs as sliding windows separated by 28 days to maintain our 28-day sampling for the full span. The benefit of the second and third strategies on C_{20} recovery is demonstrated in Figure S1 in Supporting Information S1. Lastly, standards and force models are defined in Table

S2 in Supporting Information S1, and we note that only LAGEOS-1 normal equations are generated for 1976–1993 following the analysis in Figure 2 establishing the preference for MEO-only solutions.

2.2. Truncated Singular-Value Decomposition (TSVD)

Truncated Singular-Value Decomposition (TSVD) is a type of constrained Least-Squares estimation in which regularization, or constraints, are applied along singular vector directions corresponding to small singular values in a way that eliminates data projections in those directions. This has the effect of mitigating the amplification of stochastic noise in those poorly observed directions at the expense of smearing the resolution of the true underlying state. TSVD is utilized by the Center National d'Études Spatiales (CNES) when forming their monthly GRACE gravity solutions (J.-M. Lemoine et al., 2019). The mathematical description of TSVD is developed in Equations S.1–S.9 in Supporting Information S1. The key design parameter when applying TSVD is the selection of the fraction of the trace to be retained, τ, or equivalently, the number of retained singular values, K (see Equation S.8 in Supporting Information S1). We find optimal performance (defined as best agreement with TN-14) with a value of $\tau \approx 0.995$, which results in $K = 2$ for the LAGEOS-1 56-day solutions prior to 1993, and $K = 28$ for the multi-satellite 28-day estimates 1993 and later. The resolution kernel matrix of the TSVD solution ($\mathbf{R}_r$ in Equation S.6 in Supporting Information S1) describes the level to which the true model state deviates from the identity matrix. As presented in Figure 2, the resolution kernel values are very useful for quantifying the level to which the C_{20} estimates are biased by the TSVD filter for solutions determined from different satellite sets.

2.3. TSVD Mixed-Modeling (TSVD MM)

The TSVD as described above is applied to unique sets of normal equations, resulting in C_{20} estimates that are fully independent from one another at each time step. We now discuss a Mixed-Modeling (MM) algorithm, that we combine with the TSVD estimation method, for the combined approach we call TSVD Mixed-Modeling (TSVD MM). As discussed in Section 2.1, the satellites, stations, instrumentation, etc., vary in number and quality across the data span, and in Section 3 we show that the TSVD estimation scheme provides excellent performance for the modern era, while the TSVD MM significantly improves the signal-to-noise for the earliest years. Consider classic Mixed-Modeling (MM), where it is assumed that the signal can be decomposed into fixed-effects, that is, a deterministic part, and stochastic-effects, thus, a mixed-model. The Bayesian prior on the stochastic effects is toward zero within a given covariance. This is useful when individual point samples are too contaminated to provide useful information, but collectively may provide beneficial information about group behavior. In this case, the pre-1993 months cannot be fit independently like the post-1993 months, but long-term C_{20} behavior may be extracted by fitting splines and oscillations over the full span (the fixed-effects) while also estimating individual monthly signals using Bayesian prior (stochastic-effects). Due to monthly spatial observability issues, the MM is modified by employing TSVD in forward and backward substitution inversions of stochastic effects and the inversion of the associated Shur Complement of the stochastic effects during Gaussian Elimination, thus leading to the TSVD MM least-squares scheme, described by Equations S.10-S.30 in Supporting Information S1.

In addition to the TSVD design parameter K (or τ), the TSVD MM introduces fixed-effect parameters, $\mathbf{y}_{tmm}$, and stochastic impulses, $\mathbf{x}_{tmm}$, with the stochastic signal covariance, $\mathbf{P}^{-1} = \lambda \mathbf{I}$ (all terms refer to Equation S.17 in Supporting Information S1). We define the preferred parameters as those that best meet these criteria: (a) the solution agrees well with TN-14 over the GRACE/-FO era, and (b) the stochastic component for pre-1993 has a similar character as post-1993. The first criteria follows the assumption that TN-14 provides the best possible estimates of C_{20}, while the second assumes that the deviations about the fixed-effects should be similar throughout the time span. Our optimal setup of the TSVD MM has the following parameters: (a) the fixed effects include an degree 2 polynomial with annual and semi-annual oscillations, (b) pre- and post-1993 K values of 2, and 28, respectively, consistent with the non-MM solution, and (c) pre- and post-1993 λ values of 1×10^{23} and 4×10^{21}, respectively.

2.4. Summary of Studied Scenarios

To quantify and understand the impacts of TVG modeling and various estimation strategies on J_2, we analyze the results for the following list of solutions, where the parameter list, number of satellites, and span of dates are noted:

1. CSR 5 $\times$ 5 + C_{61}/S_{61}, 5–8 satellites, 2002–2024 (current CSR solution file: C20_Long_Term.txt);
2. GSFC 5 $\times$ 5 + C_{61}/S_{61}, 5–8 satellites, 2002–2024 (TN-14);
3. CSR 3 $\times$ 3 + C_{40}, 2–8 satellites, 1976–2012 (original (Cheng et al., 2013) solution file: C20_1976_2011.txt);
4. GSFC 3 $\times$ 3 + C_{40}, 2 satellites (LAGEOS-1 and Starlette), 1994–2024;
5. GSFC 3 $\times$ 3 + C_{40}, 5–8 satellites, 1994–2024;
6. GSFC C_{20}-only, 1–3 MEO satellites, 1976–2024;
7. GSFC TSVD, 1–3 MEO satellites, 1976–2024;
8. GSFC TSVD MM, 1–3 MEO satellites, 1976–2024.

As a reminder, Scenario 2 is treated as the Truth, and the results presented below will support our selection of Scenario 8 as our recommended long-term solution.

3. Results

As summarized in Figure 2, we have successfully developed a method to recover J_2 without the use of TVG models through the application of TSVD to MEO satellites only. This is demonstrated by the excellent agreement between TN-14 and our TSVD/MEO time series in Figures 2a and 2c, even for the scenario where only LAGEOS-1 data is used (2c). The mathematical case for excluding the LEO satellites from the solution is clear when examining Figures 2b and 2d, which presents the TSVD resolution kernels for C_{20} (see Section 2.2 and $\mathbf{R}_r$ in Equation S.6 in Supporting Information S1). A perfect, unregularized resolution kernel with no leakage would have a value of one for C_{20} and zero for all other coefficients, so the deviation from this is a measure of how much leakage/smoothing is introduced via the TSVD. When analyzing resolution kernels for the 8 satellites available in January 2024 (Figure 2b), we report C_{20} values of 0.75, 0.76, and 0.93 for the 5 LEO, 8-satellite, and 3 MEO cases, respectively. Additionally, significantly more leakage (i.e., non-zero values) is clearly visible for the 8-satellite case for coefficients C_{40}, C_{60}, C_{80}, C_{90}, and $C_{10,0}$. When only considering the satellites available in 1976 (Figure 2d), the differences between the all satellites and MEO-only are smaller, with the 2-satellite and LAGEOS-1 C_{20} values of 0.84 and 0.79, respectively. While the C_{20} value slightly prefers the 2-satellite solution, integrating the rest of the coefficients for both scenarios yields a smaller value for LAGEOS-1, with $C_{10,0}$ being a major contributor. We also note that the Starlette-only kernel shows far more leakage between coefficients than is seen for LAGEOS-1. Following the kernel analysis and the improved agreement with TN-14, we decided to use all available MEO satellites when producing our long-term C_{20} estimates. From a physical standpoint, the reduction in crosstalk between C_{20} and the coefficients makes sense for the higher altitude MEO satellites, as they are low enough to be sensitive to C_{20}, but high enough to have reduced sensitivity to the other coefficients, as the gravitational acceleration is inversely proportional to the square of the distance.

Having successfully demonstrated our method to produce a C_{20} solution that agrees with TN-14 without the use of TVG models, we now present results back to 1976. Applying the TSVD approach summarized in Section 2.2 and presented in Figure 2 results in the light blue line shown in Figure 3. The high level of noise observed for the earlier years motivates the introduction of the TSVD MM (Section 2.3), and results in our recommended long-term solution shown as the dark blue line. We note that the uncertainty time series in Figure 3c is determined by scaling the formal uncertainties to match the standard deviation of the differences to TN-14.

We conclude our analysis by presenting in Figure 4 key J_2 statistics for the full suite of solutions considered for three different time intervals that span 1976 to 2024, which are informed by the availability of the various solutions (see Section 2.4). The comparisons are presented in terms of the best-fit trend and annual periodic regression parameters, and the root mean square (RMS) of the residual that remains after the J_2 time series has the trend and seasonal periodics (annual and semi-annual) removed. Beginning with the GRACE-era time interval of 2002–2024, we see in Figure 4 that both the TSVD and TSVD MM solutions provide excellent agreement in trend, annual amplitude, and RMS with the TN-14 solution that we regard as the "Truth." We note that the reduction in noise (i.e., RMS) for the earlier years of our recommended TSVD MM relative to TSVD does not have a notable impact on the fit parameters across time intervals.

In contrast to the TSVD MM, Figure 4 shows that 3 $\times$ 3 estimates produce large differences to TN-14 in terms of both trend and annual amplitude (also in Figure 2). Extending the analysis to earlier time intervals shows that the 3 $\times$ 3 consistently disagrees with the recommended TSVD MM in both trend and annual amplitude. We believe this consistent disagreement highlights the systematic issues associated with the original (Cheng et al., 2013)

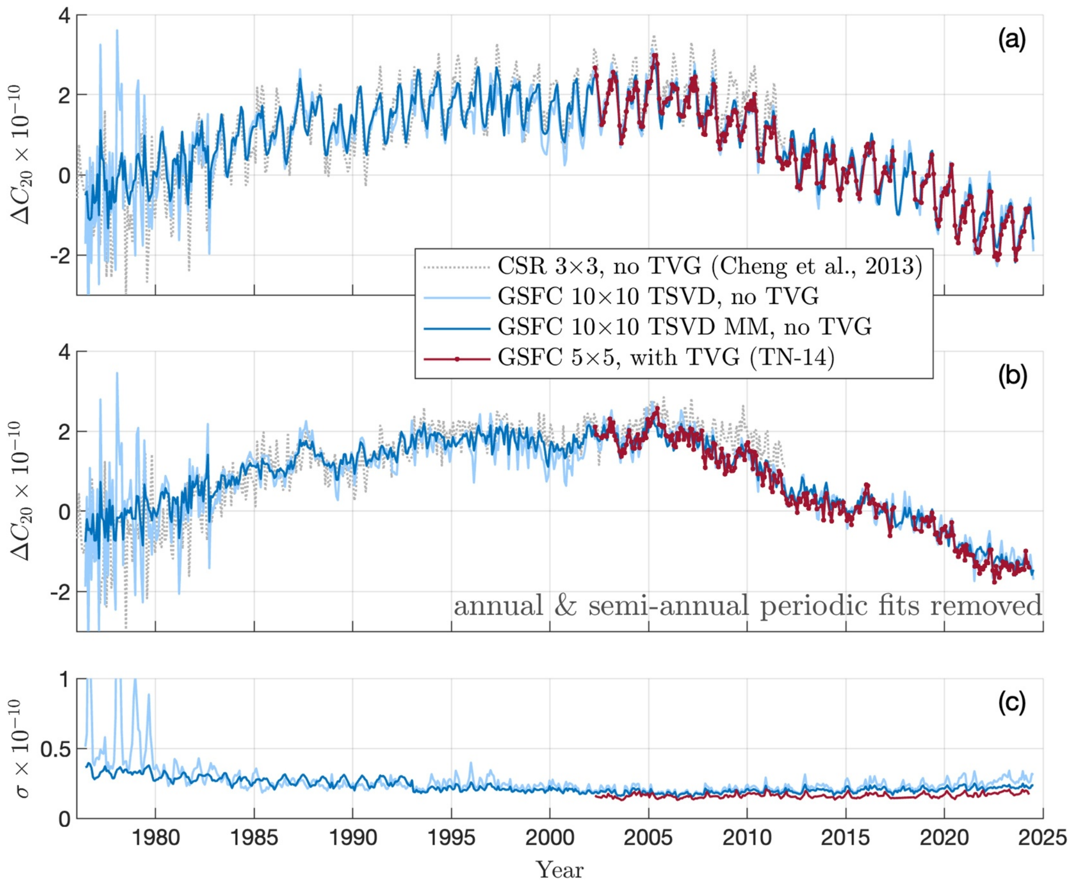

Figure 3. (a) ΔC_{20} solutions for 1976–2024. (b) Same as (a) except the annual and semi-annual period fits have been removed. (c) Calibrated solution uncertainties. The relative biases between the (Cheng et al., 2013) and TN-14 solutions are consistent with Figure 1a.

solution and the current CSR long-term solution prior to 2002. We note that the disagreement is reduced earlier in the time series, presumably because the TVG signals that impact the J_2 estimation were much smaller due to less ice melt during the pre-GRACE era (Otosaka et al., 2023). Though the earlier differences are smaller, they are statistically significant, with the TSVD MM and (Cheng et al., 2013) producing 1976–1991 trends of $-3.1 \pm 0.2 \times 10^{-11}$/year and $-3.7 \pm 0.3 \times 10^{-11}$/year, respectively (2-$\sigma$ statistical uncertainties reported). As previously discussed, the J_2 rate for this earliest span has been of considerable interest in the scientific literature,

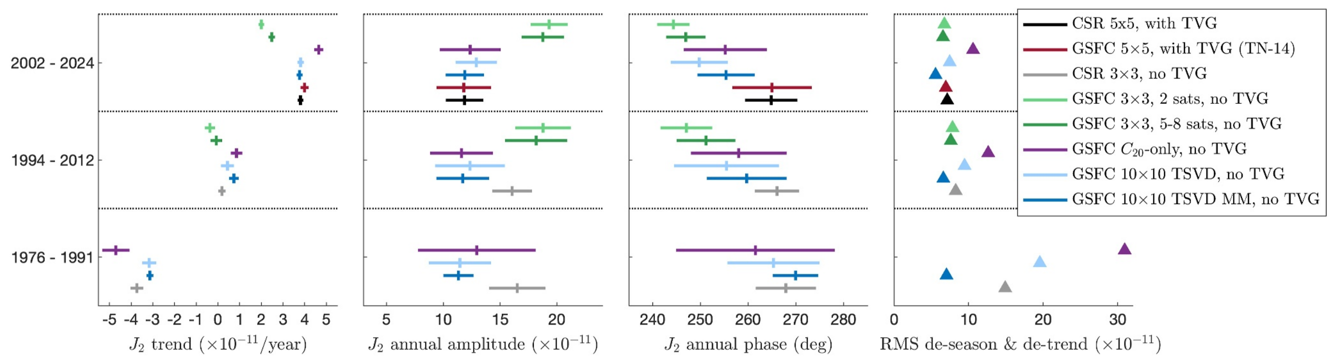

Figure 4. Statistics for different J_2 solutions for three different time spans: Apr 2002 through Dec 2023 (2002–2024), Jan 1994 through Dec 2011 (1994–2012), Apr 1976 through Dec 1990 (1976–1991). The annual amplitude, A, and phase, ϕ, are defined by $A\cos(2\pi t - \phi)$, where t is time relative to Jan 1. 2-σ statistical uncertainties are shown. See Section 2.4 for J_2 solution details. GSFC 5 × 5 (TN-14) is treated as the "Truth" and TSVD MM is the recommended long-term solution.

in particular for GIA modeling and validating pre-GRACE estimates of ice melt and its contribution on sea level rise.

We also considered a C_{20}-only solution, with Figure 4 showing that it is clearly not viable due to its inability to replicate the TN-14 trend and its very large RMS relative to the recommended TSVD MM. And while the TSVD MM demonstrates consistent stochastic behavior across all considered time spans, we acknowledge that the reduced RMS for 2002–2024 may be indicative that some damping of the month-to-month signal is occurring due to the regularization inherent to the technique.

4. Conclusions

We have successfully developed a new methodology to apply SLR tracking data to the accurate recovery of J_2/C_{20} without the need for TVG models. This was accomplished with the combination of two strategies: (a) the application of TSVD, and (b) only using the MEO (highest altitude) SLR satellites available. Additionally, we improved the stochastic (i.e., noise) behavior of the J_2 solution for the earliest years of the time series with three key strategies: (a) increasing the SLR processing arc length from 7 to 56 days, (b) applying simple station measurement bias modeling, and (c) co-estimating fixed effects along with the month-to-month variability with the TSVD MM. As demonstrated in Figures 2–4, the recommended TSVD MM has excellent agreement with the well-established TN-14 solution during the GRACE era, while Figures 3 and 4 show the improved stochastic behavior for TSVD MM relative to the TSVD alone. Of significance is the modified J_2 trend for the earliest interval, 1976–1991, for which (Cheng et al., 2013) yields $-3.7 \pm 0.3 \times 10^{-11}$/year, while our recommended TSVD MM product reports $-3.1 \pm 0.2 \times 10^{-11}$/year. This difference is large enough to impact conclusions of previous studies that relied upon the CSR long-term J_2 product. The geophysical and climate-related (i.e., ice melt) implications of our improved product is beyond the scope of this work and will be explored in a separate study. The analyses and conclusions of this paper are only relevant for the recovery of J_2, and the applicability of these methods to the recovery of other individual coefficients or a low degree field (e.g., 5×5) has not been thoroughly investigated.

Data Availability Statement

The current CSR C_{20} solution file is available at https://filedrop.csr.utexas.edu/pub/slr/degree_2/. The original file distributed with (Cheng et al., 2013) is no longer publicly available. SLR normal points data for all SLR satellites are distributed by CDDIS at https://cddis.nasa.gov/Data_and_Derived_Products/SLR/Normal_point_data.html. The standard normal point data is used for all data, except for LAGEOS-1 1976–1990 which is available at https://cddis.nasa.gov/archive/slr/data/fr/lageos1/npt/lageos1_GSFC_npt.1976_1990.Z The recommended ILRS station biases are available at https://cddis.nasa.gov/Data_and_Derived_Products/SLR/slrf_2020.html. TN-14 is available at https://podaac.jpl.nasa.gov/gravity/gracefo-documentation. The new GSFC C_{20} solution file presented in this study is available at https://earth.gsfc.nasa.gov/geo/data/slr/.

Acknowledgments

This work was funded by the NASA Earth Surface and Interior Grant NNH22ZDA001N-ESI and the NASA GRACE-FO Science Data System. We gratefully acknowledge the expertise of our NASA GSFC colleagues D. Rowlands, J. Nicholas, N. Zelensky, and D. S. Chinn, whose prior work was foundational to this study through the development of the GEODYN software and other SLR processing capabilities.

References

Agnew, D. C. (2024). A global timekeeping problem postponed by global warming. *Nature*, *628*(8007), 333–336. https://doi.org/10.1038/s41586-024-07170-0

Argus, D. F., Peltier, W. R., Blewitt, G., & Kreemer, C. (2021). The viscosity of the top third of the lower mantle estimated using GPS, GRACE, and relative sea level measurements of glacial isostatic adjustment. *Journal of Geophysical Research: Solid Earth*, *126*(5), e2020JB021537. https://doi.org/10.1029/2020JB021537

Cheng, M., & Ries, J. (2017). The unexpected signal in GRACE estimates of C20. *Journal of Geodesy*, *91*(8), 897–914. https://doi.org/10.1007/s00190-016-0995-5

Cheng, M., Tapley, B. D., & Ries, J. C. (2013). Deceleration in the Earth's oblateness. *Journal of Geophysical Research: Solid Earth*, *118*(2), 740–747. https://doi.org/10.1002/jgrb.50058

Flechtner, F. (2007). AOD1B product description document for product release 05. Retrieved from https://earth.esa.int/eogateway/documents/20142/37627/GRACE-AOD1B-PDD-20070413.pdf

Lemoine, F. G., Klosko, S. M., Cox, C. M., & Johnson, T. J. (2006). Time-variable gravity from SLR and DORIS tracking. Retrieved from https://ilrs.gsfc.nasa.gov/lw15/docs/presents/Monday1420.pdf

Lemoine, J.-M., Biancale, R., Reinquin, F., Bourgogne, S., & Gégout, P. (2019). CNES/GRGS RL04 Earth gravity field models, from GRACE and SLR data. (GFZ Data Services). https://doi.org/10.5880/ICGEM.2019.010

Loomis, B. D., Rachlin, K. E., & Luthcke, S. B. (2019). Improved Earth oblateness rate reveals increased ice sheet losses and mass-driven sea level rise. *Geophysical Research Letters*, *46*(12), 6910–6917. https://doi.org/10.1029/2019gl082929

Loomis, B. D., Rachlin, K. E., Wiese, D. N., Landerer, F. W., & Luthcke, S. B. (2020). Replacing GRACE/GRACE-FO C30 with satellite laser ranging: Impacts on Antarctic Ice Sheet mass change. *Geophysical Research Letters*, *47*(3), e2019GL085488. https://doi.org/10.1029/2019GL085488

Mitrovica, J. X., Hay, C. C., Morrow, E., Kopp, R. E., Dumberry, M., & Stanley, S. (2015). Reconciling past changes in Earth's rotation with 20th century global sea-level rise: Resolving Munk's enigma. *Science Advances*, *1*(11), e1500679. https://doi.org/10.1126/sciadv.1500679

Nerem, R. S., & Wahr, J. (2011). Recent changes in the earth's oblateness driven by Greenland and Antarctic ice mass loss. *Geophysical Research Letters*, *38*(13). https://doi.org/10.1029/2011GL047879

Otosaka, I. N., Shepherd, A., Ivins, E. R., Schlegel, N.-J., Amory, C., van den Broeke, M. R., et al. (2023). Mass balance of the Greenland and Antarctic ice sheets from 1992 to 2020. *Earth System Science Data*, *15*(4), 1597–1616. https://doi.org/10.5194/essd-15-1597-2023

Ries, J. (2024). Personal communication.

Shahvandi, M. K., Adhikari, S., Dumberry, M., Mishra, S., & Soja, B. (2024). The increasingly dominant role of climate change on length of day variations. *Proceedings of the National Academy of Sciences*, *121*(30), e2406930121. https://doi.org/10.1073/pnas.2406930121

Sośnica, K., Jäggi, A., Meyer, U., Thaller, D., Beutler, G., Arnold, D., & Dach, R. (2015). Time variable Earth's gravity field from SLR satellites. *Journal of Geodesy*, *89*(10), 945–960. https://doi.org/10.1007/s00190-015-0825-1

Tucker, E. S., Nerem, R. S., & Loomis, B. D. (2022). Simulation of a future SLR satellite to improve low-degree gravity estimates. *Journal of Geophysical Research: Solid Earth*, *127*(12), e2022JB025743. https://doi.org/10.1029/2022JB025743

Zelensky, N. P., Lemoine, F. G., Chinn, D. S., Melachroinos, S., Beckley, B. D., Beall, J. W., & Bordyugov, O. (2014). Estimated SLR station position and network frame sensitivity to time-varying gravity. *Journal of Geodesy*, *88*(6), 517–537. https://doi.org/10.1007/s00190-014-0701-4